Discontinuous Pulse Width Modulation Algorithm for Single-phase Grid-connected Inverter

Xi-jun YANG[1], Frede Blaabjerg[2], Hao QU[1], Hou-jun Tang[1]
[1] Key Lab. of Power Transmission and Conversion Control (Ministry of Education), [2]Dept. of Energy Technology
[1]Shanghai Jiao Tong University, [2]Aalborg University
[1]Shanghai 200240, [2]Aalborg 9220
[1]P.R. CHINA, [2]DENMARK
[1]youngxijun@163.com，[2]fbl@et.aau.dk

Abstract: -Single-phase grid-connected inverter (GCI) is a kind of single-phase voltage source converter (VSC), and as the indispensable tie unit between different power supplies, it is widely used in the fields of wind generation and solar PV generation. In the paper, as first, on the basis of the concept of the discontinuous pulse-width modulation (DPWM) for three-phase VSI, a new DPWM of single-phase GCI is presented by means of zero-sequence component injection. Then, the transformation from stationary frame (abc) to rotating frame (dq) is designed after reconstructing the other orthogonal current by means of one order all-pass filter. Finally, the presented DPWM based single-phase GCI is established, analyzed and simulated by means of MATLAB/SIMULINK. The simulation results show the validation of the above modulation algorithms, and the DPWM based single-phase GCR has reduced power loss and increased efficiency.

Key-Words: - Voltage source inverter, Grid-connected inverter, Zero-sequence component, Discontinuous pulse width modulation, abc-dq coordinate transformation, Slide mode control

1 Introduction

The traditional single-phase voltage source converter (VSC) can work as different power electronic converter (PEC), including single-phase voltage source inverter (VSI). When VSI is employed as tie unit between different power supplies, it becomes grid-connection inverter (GCI) .

As a PEC, in the process of operation, it is inevitable that the power devices in GCI will produce power losses, which can reduce the overall efficiency and do harm to their service lives. Generally, the power losses can be divided into dynamic losses and static losses. The former includes turning-on loss and turning-off loss, which accounts for a large proportion and goes up with the increase of the switching frequency. The latter includes on-state loss and off-state loss, where on state loss is related to on resistance and duty cycle, and off state loss can be neglected due to the small percentage. Of course, the power losses are subject to the switching stress, including switching voltage and switching current.

Many efforts are plunged to make clear the heating mechanism, mathematical model, equivalent circuit and computation method. Essentially, in order to degrade the power losses, it is helpful to modify the modulation algorithm without the sacrifice of the waveform synthesis. Switching loss reduced PWM, i.e. discontinuous PWM has obtained much investigation for three-phase VSC with many outcomes [1-10], including APF [11-12]. The main principle is to inject an appropriate zero-sequence component into the original sinusoidal target function and gain a discontinuous or piecewise target function. There are durations where the maximum duty cycle is 1 or the minimum duty cycle 0. The best arrangement is to make such durations fall into the neighborhood of peak current in order to decrease the resultant losses to a maximum extent.

In the paper, the above concept is introduced to single-phase GCI. In order to obtain d and q axis components in dq coordinate, the general method is to

reconstruct an orthogonal input current by phase shifting and 2x2 rotating transformation matrix[13-16]. A first-order all-pass filter is used which can effectively create the orthogonal current signals[17-18]. According to the above descriptions, a new DPWM based single-phase GCI is investigated and simulated in the paper. The gained results prove that the new DPWM based single-phase GCI features reduced power losses.

2 Principle of DWPM

A. The circuit topologies

The power stage of single-phase GCI is shown in Fig.1(a), where reverse conduction switches S1 and S4 constitute the first arm, and S3 and S6 constitute the second arm, and each reverse conduction switch consists of an IGBT and an anti-paralleled free-wheeling diode. The grid filter is of LCL type or L type.

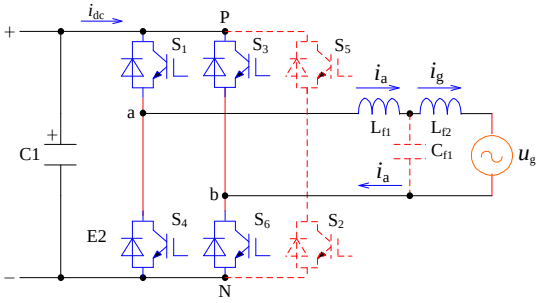

Fig.1 Power stage of single-phase GCI

B. The presented DPWM

As for single-phase GCI, there are two basic device grouping methods. Reverse conduction switches S1 and S6，S3 and S4 are severally in a group, named grouping I, which merely can use double polarity continuous SPWM;

Reverse conduction switches S1 and S4，S3 and S6 are severally in a group, named grouping II, which can use double polarity continuous SPWM, the above said DPWMs, and the other PWMs with zero-sequence component injection.

As for grouping II, the phase difference between the two fundamental target functions on the two midpoint of the two arms can be (0, π].

Within any power electronic converters, it is inevitable for each power device to produce switching-on loss, switching-off loss, on-state loss, and the omitted off-state loss. A generalized loss expression of each power device was given in reference [19].

$$P_L = g(\bar{U}_{ds}, \bar{I}_d)\, \bar{f}_s \tag{1}$$

where $\bar{U}_{ds}$ indicates the average on-state voltage drop; $\bar{I}_d$ the average on-state current; $\bar{f}_s$ the average switching frequency; P_L the monotonous increasing function of $\bar{U}_{ds}$ and/or $\bar{I}_d$.

Equation (18) shows the importance to reduce $\bar{f}_s$ and the necessity to move the non-switching zone to the maximum conduction current zone, in order to reduce the switching loss to a great extent. Another critical point is to make all of the reverse conduction switches have the same power loss as the best possible.

The concept of DPWM has already been investigated and applied in three-phase VSC by use of appropriate zero-sequence components[1-4,11-12]. Obviously, the practice can be introduced to single-phase VSC.

Given three-phase symmetrical sinusoidal functions as the original target functions

$$\begin{cases} u_a = m\sin(\omega_i t) \\ u_b = m\sin(\omega_i t - \alpha) \\ u_c = m\sin(\omega_i t + \alpha) \end{cases} \tag{2}$$

where m is modulation index, $0 \le m \le 1$.

In Equation (2), the initial phase is zero. Actually, when the three-phase VSC works as three-phase GCI, the initial phase and m are determined by the working conditions.

$\max(u_a, u_b, u_c)$ and $\min(u_a, u_b, u_c)$ can be decomposed as DC component, zero-sequence components and even order harmonic components.

In addition, the third, ninth, fifteenth order harmonic components and even DC component can also be taken into consideration. The linear combination of the above elements can be used as the final zero-sequence component.

The even order harmonic components should be eliminated to make the resultant target function have the form of pure zero-sequence component. An alternative zero-sequence component combination can be stated as [1-6]

$$u_0 = -k \cdot \max(u_a, u_b, u_c) - (1-k)\min(u_a, u_b, u_c) + 2k-1 \quad (3)$$

where k is an arbitrary pulse train, $k = 1$ or 0.

Then the new target functions of single-phase GCI are obtained as

$$\begin{cases} u_a' = u_a + u_0 \\ u_b' = u_b + u_0 \end{cases} \quad (4)$$

The existence of zero-sequence component changes the waveform of the original target function. Equation (4) implies the non-switching zone for a specific power device within a mains period, due to the occurrence of 1 or 0 for duty ratio.

The primary task is to make k vary with the phase displacement between mains voltage and mains current, and to arrange the non-switching zone fall into the neighborhood of peak mains current in order to minimize the switching losses.

C. The dq coordinate transformation

In theory, well-designed PI regulator has better control results in dq coordinate than in abc coordinate, due to it can acquire infinite loop gain and the resultant zero steady state error at the fundamental frequency.

Unlike three-phase GCI, single-phase GCI has to establish its own abc-dq coordinate transformation.

An easy approach is to reconstruct the required orthogonal phase current with respect to the original phase current by directly shifting the initial phase of the original current by 1/4 mains period dynamically, or by first-order all-pass filter to create the required orthogonal signal. The first-order all-pass filter features unchanged magnitude of the filtered original signal while the initial phase is shifted. The transfer function of the first-order all-pass filter is given as

$$G_f = \frac{\omega_i - s}{\omega_i + s} \quad (5)$$

As a result, the desired two components in αβ stationary coordinate are built up. Then conventional practice can be used to complete the αβ-DQ transformation.

The αβ-DQ transformation matrix is

$$T = \begin{bmatrix} \cos(\omega_i t) & \sin(\omega_i t) \\ -\sin(\omega_i t) & \cos(\omega_i t) \end{bmatrix} \quad (6)$$

and the corresponding dq-αβ transformation matrix is

$$T^{-1} = \begin{bmatrix} \cos(\omega_i t) & -\sin(\omega_i t) \\ \sin(\omega_i t) & \cos(\omega_i t) \end{bmatrix} \quad (7)$$

3 Simulation Analysis

A. DPWM based single-phase GCI

After combined with abc-dq coordinate transformation as well as well-configured PI regulation, a simulation platform of the presented DPWM based single-phase GCI is established by means of MATLAB/SIMULINK and simulated thoroughly.

Simulation conditions: singe-phase mains voltage is 120Vrms/50Hz, the desired DC voltage is 385V, the rated load power is 2.0kW, and the boost inductance is 5.0mH, with DC resistance of 0.01Ω.

Simulation platform of single-phase GCI is shown in Fig.2, where the power stage is in Fig.2(a) , the coordinate transformation in Fig.2(b), the PI regulation in Fig.2(c), the k generation in Fig.7(d), the DPWM generation in Fig.2(e).

The frequency of k is three times of the mains frequency. Because the specified IGBT is in off state within the 60° interval after the peak mains current, its initial phase is 30° leading to the mains current.

When the single-phase GCI works at PF=1, its initial phase is 30° leading to the mains voltage/mains current. The first-order all-pass filter can be used to gain the initial position of k.

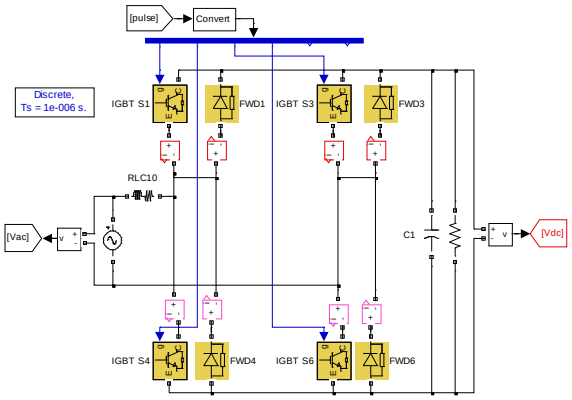

(a) Power stage of the single-phase GCI

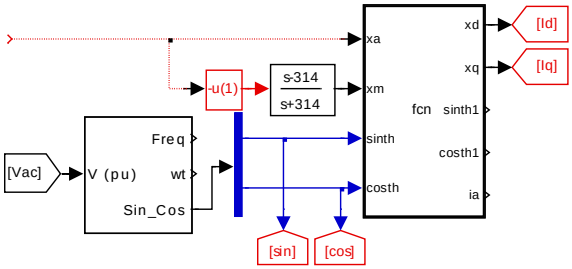

(b) Coordinate transformation of the single-phase GCI

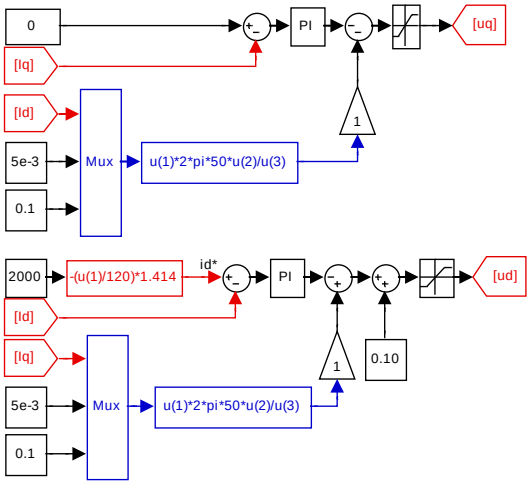

(c) PI regulation of the single-phase GCI

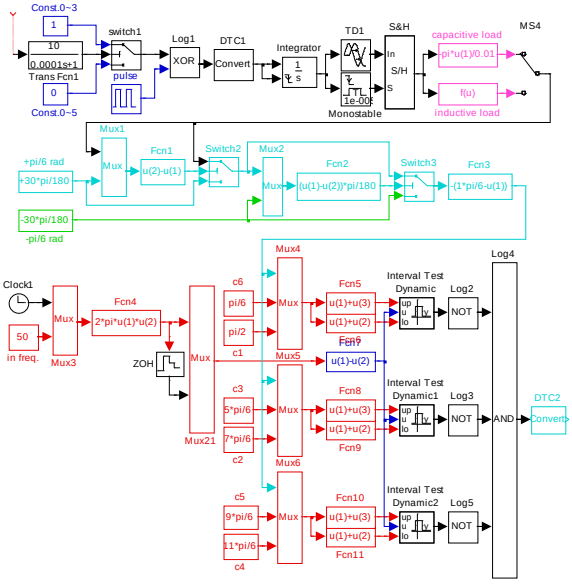

(d) k generation of the single-phase GCI

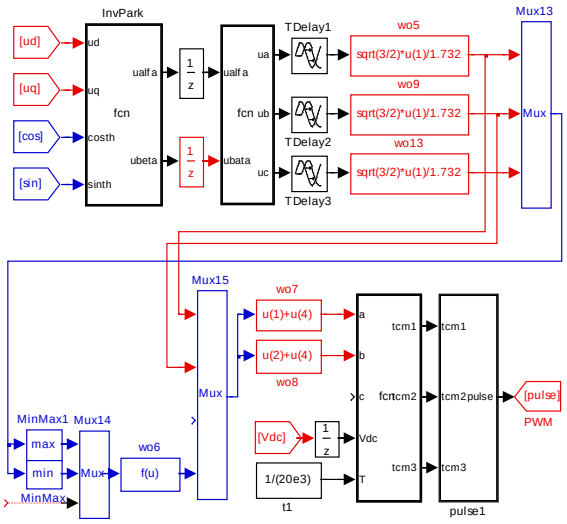

(e) DPWM generation

Fig.2 Simulation platform of single-phase GCI, based on DPWM (a) the power stage, (b) the coordinate transformation, (c) the PI regulation, the k generation, (d) k generation of the single-phase GCI, (e) the DPWM generation

Fig.3 shows the waveforms of pulse train k, zero-sequence component u_0, the fundamental function u_0, and the final target function.

Fig.4 shows the waveforms of mains current and currents of IGBT S1, S2, S3 and S4.

Fig.5 shows the waveforms of mains current and currents of free-wheeling diode FRD1, FRD2, FRD3 and FRD4.

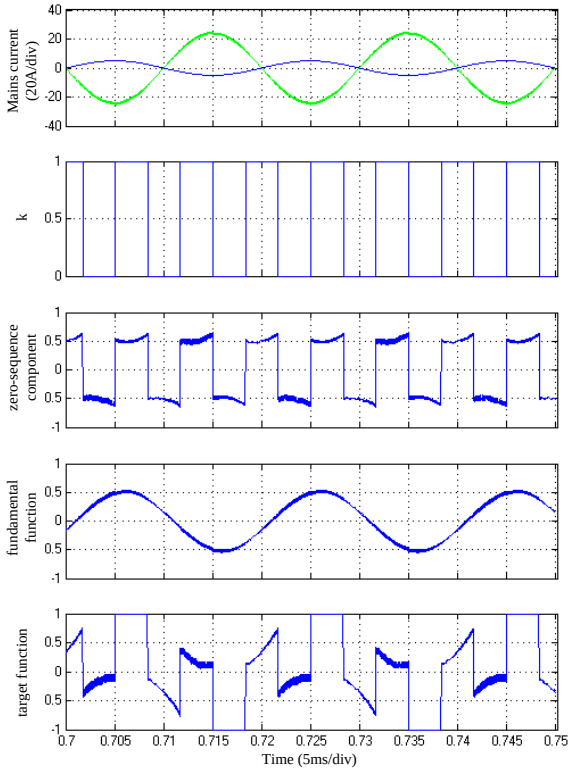

Fig.3 Waveforms of pulse train k, zero-sequence

component u_0, the fundamental function u_0, and the final target function, based on the presented DPWM

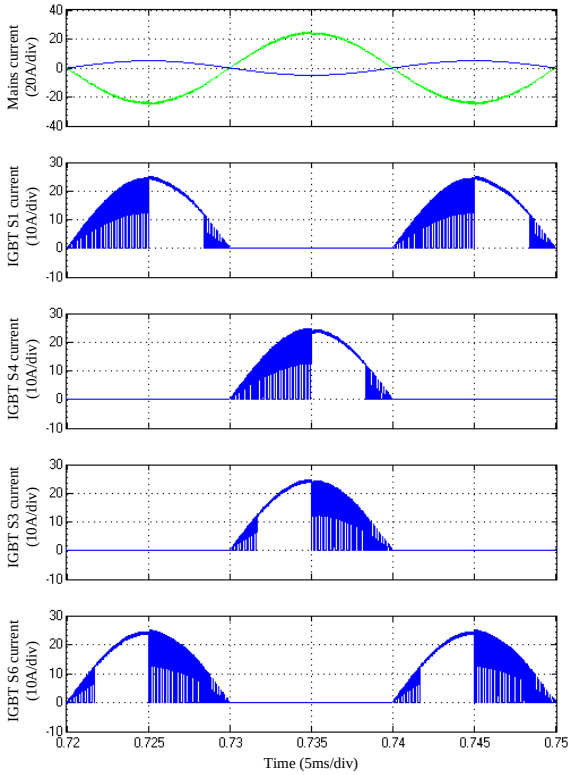

Fig.4 Waveforms of mains current and currents of IGBT S1, S2, S3, S4, based on DPWM, based on the presented DPWM

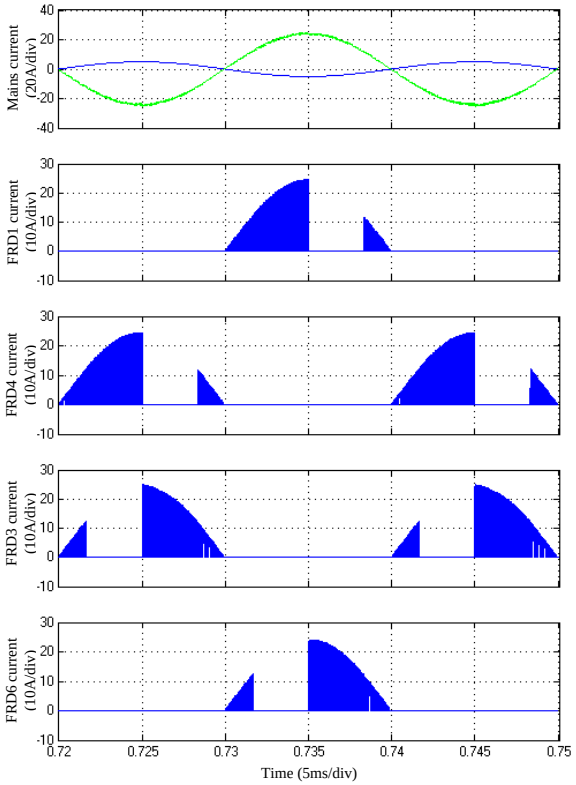

Fig.5 Waveforms of mains current and currents of free-wheeling diode FRD1, FRD2, FRD3 and FRD4, based on the presented DPWM

As for the presented DPWM, it is unlikely to make the non-switching zone distributed symmetrically on both side of peak mains current, or else, there can be more non-switching zones, and the current waveform will get more complicated. It has the following characteristics:

(1) The four IGBTs are constantly conducted within the non-switching zone, but the four FWDs are constantly non-conducted within the non-switching zone, bringing about almost the identical switching losses, nevertheless the conduction losses are slightly different due to unsymmetrical current details;

(2) IGBT S1 and S4 constitute the first arm, and the non-switching zone of S1 falls into the interval [90°, 150°], and that of S4 [270°, 330°]. IGBT S3 and S6 constitute the second arm, and the non-switching zone of S3 falls into the interval [210°, 270°], and that of S6 [30°, 90°]; Accordingly, the non-switching zone of FRD1 [270°, 330°], FRD4 [90°, 150°], FRD3 [30°, 90°], and FRD6 [210°, 270°];

(3) The current waveforms of FWD1 and S4, FWD4 and S1, FWD3 and S6, FWD6 and S3 are complementary, respectively, and the summations of them appear as half period sinusoidal waveforms.

B. SPWM single-phase GCI

In order to make clear comparisons, the traditional continuous SPWM based single-phase GCI is simulated under the same conditions.

Fig.6 shows the waveforms of mains current and currents of IGBT S1, S2, S3 and S4.

Fig.7 shows the waveforms of mains current and currents of free-wheeling diode FRD1, FRD2, FRD3 and FRD4.

The presented DPWM features the same switching number and roughly symmetrical current distribution. Perhaps it is a promising PWM for single-phase GCI.

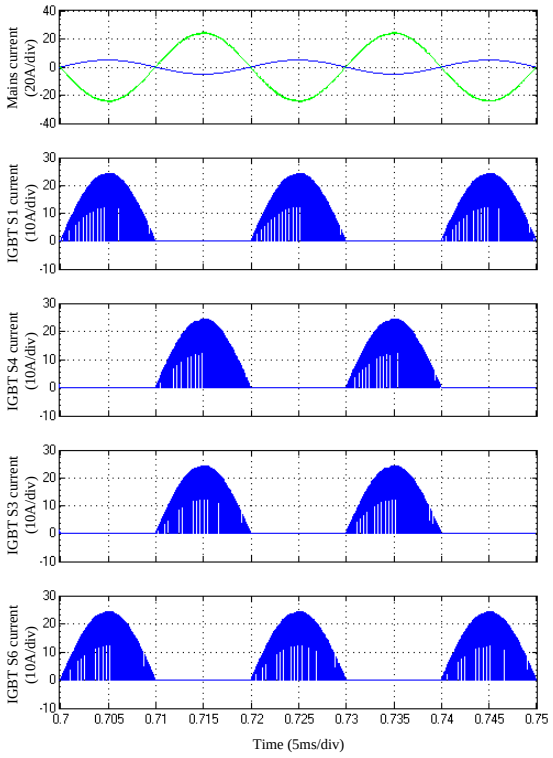

Fig.6 Waveforms of mains current and currents of IGBT S1, S2, S3, S4, based on the SPWM

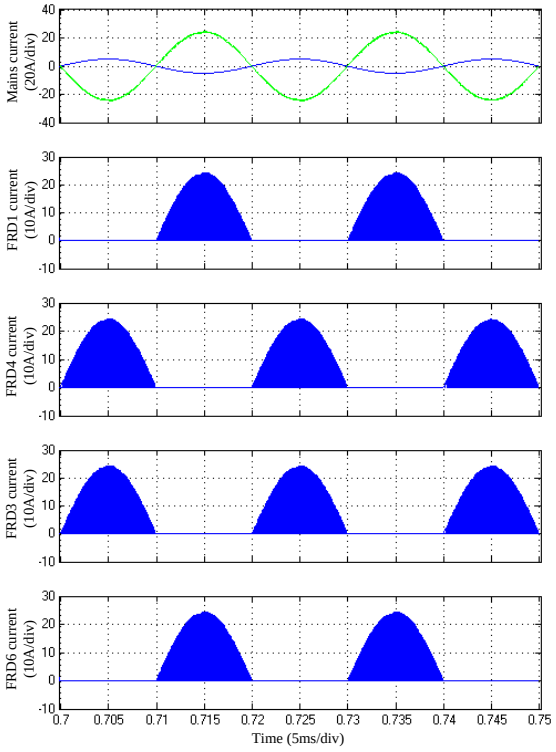

Fig.7 Waveforms of mains current and currents of free-wheeling diode FRD1, FRD2, FRD3 and FRD4, based on the SPWM

V. Loss Calculation

Assuming the carrier frequency is all the same, different modulation algorithm can lead to different static losses and dynamic losses, which can be formulated, calculated and compared.

A. The continuous SPWM

Take the device grouping I as instance, when the single-phase GCI reaches the steady state, with respect to the mains voltage, the target function can be written as

$$u_a = m_a \sin(\omega t - \theta_i) \quad (8)$$

where the modulation m_a and the initial phase θ_i depend on the working conditions.

Due to the symmetry of circuit and control, the four IGBTs have the same power losses nearly, so do the four FWDs. The current waveforms through S1 and S6, S3 and S4 are identical roughly, respectively. The current waveforms through S1 (S6) and S3 (S4) are different only in phase.

Take power device S1 for instance, the average on-state loss can be derived as

$$\frac{1}{2\pi}\int_0^{\pi} \frac{1-u_a}{2} I_{im}\sin(\omega t)\cdot U_{ce(sat)}@[I_{im}\sin(\omega t)]d\omega t \quad (9)$$

where I_{im} is the magnitude of mains sinusoidal current, $U_{d(sat)}$ is the instantaneous IGBT saturation voltage drop corresponding to the mains current.

The average switching loss is

$$\sum_{n=1}^{0.01 f_c} (E_{on}+E_{off})[@I_{im}\sin(\quad)_i \quad _c) \quad (10)$$

where E_{on} and E_{off} are the energy consumption during every turning on and every turning off, respectively, f_c is the carrier frequency.

Take free-wheeling diode FWD4 for instance, the average on-state loss can be derived as

$$\frac{1}{2\pi}\int_0^{\pi} \frac{1-u_a}{2} I_{im}\sin(\omega t)\cdot U_{ce(sat)}@[I_{im}\sin(\omega t)]d\omega t \quad (11)$$

The average switching loss is

$$\sum_{n=1}^{0.01 f_c} E_{err}@[I_{im}\sin(\quad)_o \quad _c] \quad (12)$$

where E_{err} the energy consumption during every reverse recovery.

B. The presented DPWM

The presented switching-number reduced DPWM can only employ the device grouping II. When the single-phase GCI reaches the steady state, with respect to the mains voltage, the target function can be written as

$$\begin{cases} u_a' = m_a \sin(\omega t - \theta)_i + u_o \\ u_b' = m_b \sin(\omega t - \alpha - \theta)_i + u_o \end{cases} \quad (13)$$

The average on-state loss of power device S1 is

$$\frac{1}{2\pi}\int_0^{\pi}\frac{1+u_a'}{2}I_{im}\sin(\omega_i t)\cdot U_{ce(sat)}@[I_{im}\sin(\omega_i t)]d\omega_i t \quad (14)$$

The average on-state loss of power device S4 is

$$\frac{1}{2\pi}\int_{\pi}^{2\pi}\frac{1-u_a'}{2}I_{im}\sin(\omega_i t)\cdot U_{ce(sat)}@[I_{im}\sin(\omega_i t)]d\omega_i t \quad (15)$$

The average on-state loss of power device S3 is

$$\frac{1}{2\pi}\int_{\pi}^{2\pi}\frac{1+u_b'}{2}I_{im}\sin(\omega_i t)\cdot U_{ce(sat)}@[I_{im}\sin(\omega_i t)]d\omega_i t \quad (16)$$

The average on-state loss of power device S6 is

$$\frac{1}{2\pi}\int_0^{\pi}\frac{1-u_b'}{2}I_{im}\sin(\omega_i t)\cdot U_{ce(sat)}@[I_{im}\sin(\omega_i t)]d\omega_i t \quad (17)$$

The average on-state loss of FRD1 is

$$\frac{1}{2\pi}\int_{\pi}^{2\pi}\frac{1+u_a'}{2}I_{im}\sin(\omega_i t)\cdot U_{d(sat)}@[I_{im}\sin(\omega_i t)]d\omega_i t \quad (18)$$

The average on-state loss of FRD4 is

$$\frac{1}{2\pi}\int_0^{2\pi}\frac{1-u_a'}{2}I_{im}\sin(\omega_i t)\cdot U_{d(sat)}@[I_{im}\sin(\omega_i t)]d\omega_i t \quad (19)$$

The average on-state loss of FRD3 is

$$\frac{1}{2\pi}\int_0^{\pi}\frac{1+u_b'}{2}I_{im}\sin(\omega_i t)\cdot U_{d(sat)}@[I_{im}\sin(\omega_i t)]d\omega_i t \quad (20)$$

The average on-state loss of FRD6 is

$$\frac{1}{2\pi}\int_{\pi}^{2\pi}\frac{1-u_b'}{2}I_{im}\sin(\omega_i t)\cdot U_{d(sat)}@[I_{im}\sin(\omega_i t)]d\omega_i t \quad (21)$$

The average switching loss of every IGBT is

$$\sum_{n=1}^{0.01f_c/6}(E_{on}+E_{off})@[I_{im}\sin(\omega_i\cdot n/f_c)] + \sum_{n=1+0.01f_c/2}^{0.01f_c}(E_{on}+E_{off})@[I_{im}\sin(\omega_i\cdot n/f_c)] \quad (22)$$

The average switching loss of every FWD is

$$\sum_{n=1}^{0.01f_c/6}E_{err}@[I_{im}\sin(\omega_i\cdot n/f_c)] + \sum_{n=1+0.01f_c/2}^{0.01f_c}E_{err}@[I_{im}\sin(\omega_i\cdot n/f_c)] \quad (23)$$

C. Power Device loss analysis

Compared with the continuous SPWM, the presented DPWM has the following features:

(1) Power device IGBTs are in off state within interval [30°，90°] or [90°，150°], and the switching number is reduced by 1/3, leading a reduced switching loss, roughly by 40%;

(2) Power device FWDs are in on state within interval [30°，90°] or [90°，150°], and the switching number is reduced by 1/3, leading a reverse recovery loss, roughly by 40%;

Apparently, the overall switching loss decreases, but it is needed to evaluate whether the overall conduction loss decreases or not. It is very difficult to exactly calculate the overall loss using the given equations, due to the nonlinear relationship between the conduction voltage drop and conduction current.

D. Calculation instances

It is difficult to precisely calculate the power loss according to the given data of power devices, because the practical working conditions are more different with the listed test conditions in given datasheet.

Power devices from different manufactures have different performances and parameters in terms of design principle, manufacturing process and voltage/current rating.

According to the delivered power of 2.0kW, two kinds of IGBTs with anti-parallel FWDs built inside are chosen as candidate power devices. The relevant curves and data come from their respective datasheet.

(1) IPM PM25CS1D120

PM25CS1D120, produced by MITSUBISHI, which is characteristic of 25A@25°C, 1200V, one-bridge arm power module, built-in free-wheeling diode, and the relation curves are shown is Fig.8.

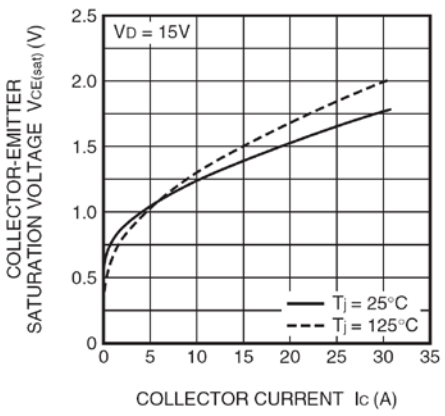

(a) $U_{ce(sat)}$ vs I_c of IGBT

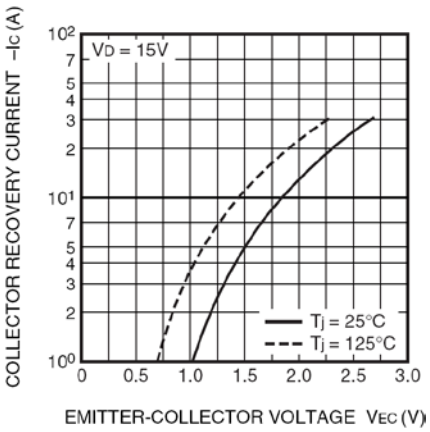

(b) I_c vs V_{EC} of FWD

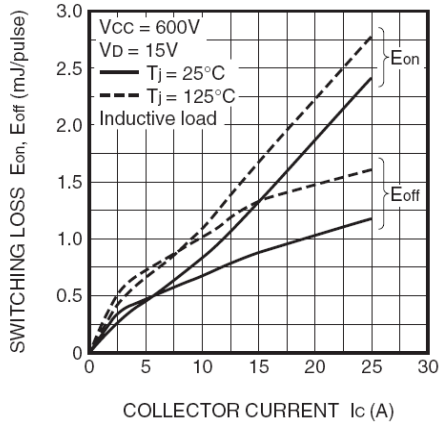

(c) ON/OFF energy of IGBT

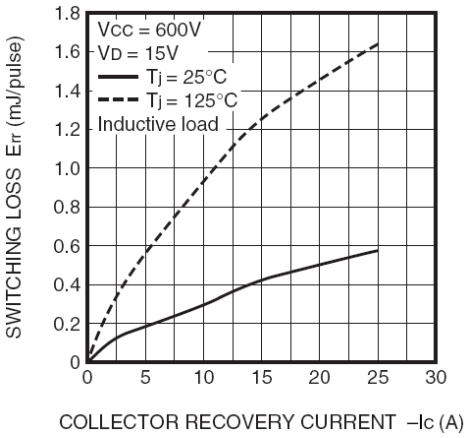

(d) Recovery energy of FWD

Fig. 8 Relation curves of PM25CS1D120

(2) IPM PM50CS1D060

PM50CS1D060, produced by MITSUBISHI, which is characteristic of 50A@25°C, 600V, 3H bridge power module, built-in free wheel diode, and the relation curves are shown is Fig.9.

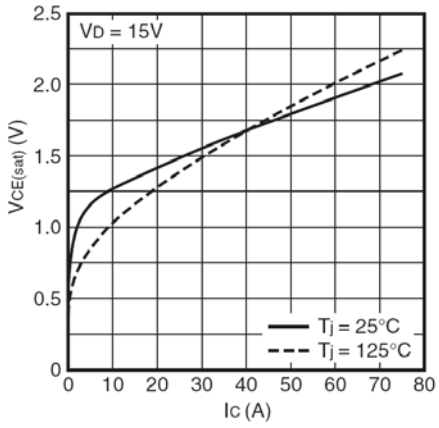

(a) $U_{ce(sat)}$ vs I_c of IGBT

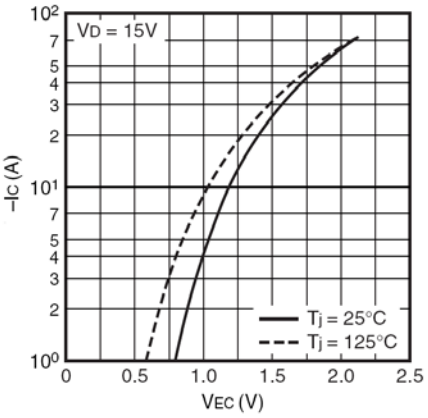

(b) Ic vs V_{EC} of FWD

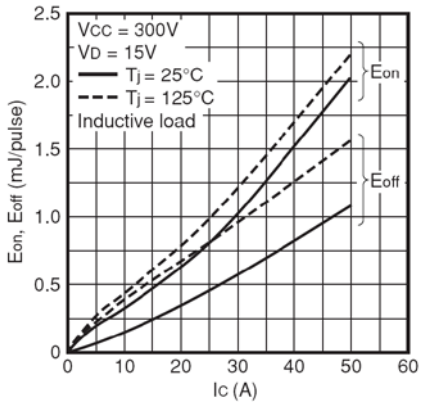

(c) ON/OFF energy of IGBT

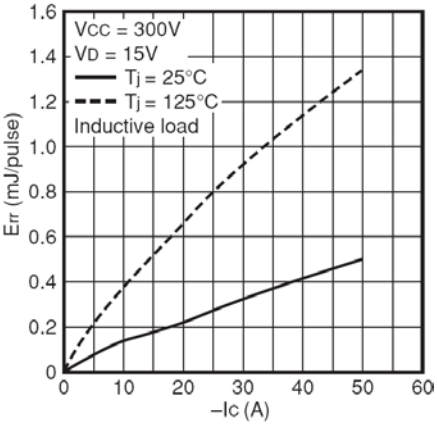

(d) Recovery energy of FWD

Fig.9 Relation curves of PM50CS1D060

Within Simulink simulation environment, the loss calculation platform is established,. At first, draw the above ten dotted characteristic curves (@125°C) into ten 1-D tables, and then look up IGBTs' conduction voltage drop, switching on loss and switching off loss as well as FWDs' forward voltage drops and reverse recovery losses according to these characteristic curves. Finally, calculate all the average losses within a mains period and fill the original data in Table 1.

It can be seen from Table 1 that as for any power devices, in case of DPWM, the total losses within the

single-phase GCI is much lower than those in case of SPWM. And the total switching loss in case of DPWM is much lower than those in case of SPWM, but the total on loss in case of DPWM is slightly higher than that in case of SPWM. In order to increase the energy-saving effect, the simulated average losses and calculated losses for the DPWM based single-phase voltage source rectifier (VSR) is shown in Table 2. The tables show the same scenario with a small difference. This is because the responding currents of IGBT and FWD in the power stage are exchange for the GCI's regeneration and VSR's consumption, and the switching characteristics are different between IGBT and FWD. It also can be seen form Table 1 and Table 2 that the power device with high blocking voltage and low conducting current has higher losses. This complies with the manufacturing principle.

V. Conclusions

In the paper, according to the discontinuous pulse-width modulation (DPWM) principle of three-phase VSC, the DPWM of single-phase GCI is presented, analyzed and simulated by means of MATLAB/SIMULINK. The DPWM is realized by use of the injection of special zero-sequence component. Simultaneously, the continuous SPWM, based single-phase GCI is simulated as comparison. The presented DPWM can reduce the whole power losses obviously for each power device, and the power losses is roughly even distributed among them. The presented DPWM has the following features: (1) Power device IGBTs are in off state within interval [30°，90°] or [90°，150°]; (2) Power device FWDs are in on state within interval [30°，90°] or [90°，150°]; (3) The average switching number is reduced by 1/3, leading a reduced switching loss, roughly by 40%; (4) The conduction losses is roughly unchanged, though in need of practical measurement.

Acknowledge

The paper is supported by the National Natural Science Foundation of China as the key project of natural science foundation (U1360203), and all the authors are very grateful for the support.

References

[1] Dae-Woong Chung, Seung-Ki Sul. Minimum-loss strategy for three-phase PWM rectifier. IEEE Transactions on Industrial Electronics[J]. 46(3): 517–526, Jun. 1999.

[2] J. A. Houldsworth, D. A. Grant. The use of harmonic distortion to increase output voltage of a three-phase PWM inverter[J]. IEEE Transactions on Industry. Application. 20(5): 1124–1228, Sept./Oct. 1984.

[3] Vladimir Blasko. Analysis of a Hybrid PWM Based on Modified Space-Vector and Triangle-Comparison Methods[J]. IEEE Transactions on Industry Applications. 33(3): 756-764, May/Jun. 1997.

[4] Andrzej M. Trzynadlowski, R. Lynn Kirlin, Stanislaw F. Legowski. Space vector PWM technique with minimum switching losses and a variable pulse rate [for VSI] IEEE Transactions on Industrial Electronics[J]. 44(2): 173-181, April 1997.

[5] Andrzej M. Trzynadlowski, Stanislaw Legowski. Comparison of the Effects of Continuous and Discontinuous PWM Schemes on Power Losses of Voltage-Sourced Inverters for Induction Motor Drives. IEEE Transactions on Power Electronics, Vol. 26 , No. 1: 182-191, JANUARY 2011.

[6] Andrzej M. Trzynadlowski, Stanislaw Legowski. Minimum-loss vector PWM strategy for three-phase inverters. IEEE Transactions on Power Electronics, Vol. 9, No. 1: 26-34, January 1994.

[7] Marcelo Cabral Cavalcanti, Edison Roberto Cabral da Silva, Antonio Marcus Nogueira Lima, Cursino Brandão Jacobina, Raimundo Nazareno Cunha Alves. Reducing losses in three-phase PWM pulsed DC-link voltage-type inverter systems. IEEE Transactions on Industry Applications, Vol. 38, No. 4: 1114-1122, July/August 20.

[8] Keliang Zhou and Danwei Wang. Relationship between space-vector modulation and three-phase carrier-based PWM a comprehensive analysis [three-phase inverters]. IEEE Transactions on Industrial Electronics, Vol. 49, No. 1: 186-196, February 2002.

[9] Shaoliang An, Shaoliang An, Yanru Zhong,

Mikihiko Matsui2. Research on a new and generalized method of discontinuous PWM strategies to minimize the switching loss. IEEE PES ISGT ASIA 2012: 1-6.

[10] A. M. Hava, R. J. Kerkman, and T. A. Lipo, A high performance generalized discontinuous PWM algorithm, IEEE Trans. Ind. Appl., vol. 34, no. 5, pp. 1059–1071, Sep./Oct. 1998.

[11] Dae-Woong Chung, Seung-Ki Sul. Reduction of Switching Losses in Active Power Filters With a New Generalized Discontinuous-PWM Strategy[J]. IEEE Transactions on Industrial Electronics. 46(3): 517-526, Jun. 1999.

[12] Lucian Asiminoaei, Pedro Rodriguez, Frede Blaabjerg, Mariusz Malinowski. Reduction of Switching Losses in Active Power Filters With a New Generalized Discontinuous-PWM Strategy[J]. IEEE Transactions on Industrial Electronics, Vol. 55, No. 1: 467-471, January 2008.

[13] Zhang R，Cardiml M，Szczesny P．A grid simulator with control of single phase power conveners in d-q rotating frame[C]. IEEE 33rd Power Electronics Specialists Conference (PESC 2002), Vol. 3, pp. 1431-1436, 2002.

[14] Salaet J，Busquets S，B0rdomu J．A new strategy for decoupling direct and quadrature currents in a rotating frame current regulator[C]. IEEE 37th Power Electronics Specialists Conference (PESC 2006), pp. 18-22, June 2006.

[15] Salaet J I, A1epuz s, Gilaben A. Comparison between two methods of DQ transformation for single phase converters control[C]. IEEE 35th Power Electronics Specialists Conference (PESC 2004), Vol. 1, pp.214-220, 2004.

[16] Miranda U A, Aredes M, Rolim L G B. A DQ synchrounous reference frame current control for single-phase converter[C]. IEEE 36th Power Electronics Specialists Conference (PESC 2005), pp.1377-1831, 2005.

[17] S. Golestan, M. Monfared, J.M. Guerrero, M. Joorabian. A D-Q synchronous frame controller for single-phase inverters[C]. 2011 2nd Power Electronics, Drive Systems and Technologies Conference, pp.317-323, Feb. 2011.

[18] B. H. Kwon, J. H. Choi, T. W. Kim. Improved single-phase line interactive UPS[J]. IEEE Transactions Ind. Electron., 48(4): 804-811, Aug. 2001.

[19] B. K. Bose. Power Electronics and Variable Frequency Drives: Technology and Applications[M]. Piscataway: IEEE Press, 1996.

Table 1 Simulated average losses and calculated losses for the DPWM-based GCI

		IGBT				FWD			switching loss subtotal (W)	on loss subtotal (W)	Total loss (W)
		on loss (W)	turning on loss (W)	turning off loss (W)	subtotal (W)	on loss (W)	Err (W)	subtotal (W)			
PM25CS1D120 x4	DPWM	35.20	39.10	28.20	102.5	18.15	28.80	46.95	96.10	53.35	149.45
	SPWM	35.10	67.95	49.20	152.3	16.38	45.90	62.28	163.05	51.48	214.53
PM50CS1D060 x4	DPWM	27.40	14.20	12.60	54.2	12.80	12.60	25.40	39.40	40.20	79.60
	SPWM	27.30	24.70	21.70	73.7	11.43	19.72	31.15	66.12	38.73	104.85

Table 2 Simulated average losses and calculated losses for the DPWM-based VSR

		IGBT				FWD			switching loss subtotal (W)	on loss subtotal (W)	Total loss (W)
		on loss (W)	turning on loss (W)	turning off loss (W)	subtotal (W)	on loss (W)	Err (W)	subtotal (W)			
PM25CS1D120 x4	DPWM	14.4	31.4	26.0	71.4	46.2	31.0	77.2	88.0	60.6	148.6
	SPWM	18.5	72.2	47.5	138.2	41.6	44.2	85.8	163.9	60.1	224.0
PM50CS1D060 x4	DPWM	11.3	10.8	10.5	32.6	31.2	14.1	55.3	45.4	42.5	87.90
	SPWM	14.4	26.4	22.0	62.8	28.2	20.2	48.4	68.6	42.6	111.2